Am J Cancer Res 2021;11(3):979-996
www.ajcr.us /ISSN:2156-6976/ajcr0120316

Original Article

EIF3m promotes the malignant phenotype of lung adenocarcinoma by the up-regulation of oncogene CAPRIN1

Xinwei Liu[1,2], Dulei Xiang[2,3], Chong Xu[3,4], Ruonan Chai[4]

[1]Department of Orthopaedics, The General Hospital of Northern Theater Command, Shenyang 110016, People's Republic of China; [2]Laboratory of Respiratory and Critical Care Medicine, The General Hospital of Northern Theater Command, Shenyang 110016, People's Republic of China; [3]Graduate Schools, Jinzhou Medical University, Jinzhou 121001, People's Republic of China; [4]Department of Respiratory Medicine, The General Hospital of Northern Theater Command, Shenyang 110016, People's Republic of China

Received August 14, 2020; Accepted October 29, 2020; Epub March 1, 2021; Published March 15, 2021

Abstract: EIF3m is the latest identified subunit of the eukaryotic translation initiation factor 3 (eIF3), however, its function in malignant tumor is rarely reported. In the current work, we observed that EIF3m was aberrant over-expressed in lung adenocarcinoma (LADC) tissues and cell lines, and the increased EIF3m level was closely related to the poor clinical outcomes of the LADC patients. The gain- and loss-of-function assays demonstrated the proto-oncogenetic potential of EIF3m *in vitro* and *in vivo*. EIF3m induced-malignant phenotype was partly mediated by the up-regulation of CAPRIN1. The biochemical analysis showed that EIF3m could bind to the 5'UTR of CAPRIN1 and positively modulate its expression at the post-transcription level. Furthermore, we identified the interaction between EIF3m and the deubiquitinase UCHL5, which stabilized and promoted the accumulation of EIF3m in LADC cells. In summary, our findings extended the knowledge about the EIF3m function and highlight the roles of the UCHL5/EIF3m/CAPRIN1 axis during the progression of LADC.

Keywords: Lung adenocarcinoma, EIF3m, CAPRIN1, UCHL5

Introduction

Lung cancer is the most serious malignant tumor threatening the life and health of humankind, with a five-year survival rate that is less than 25% [1]. Non-small cell lung cancer (NSCLC) is the major subtype of lung cancer (accounting for 85% of all lung cancer cases). NSCLC comprehends three histological subtypes, including squamous-cell carcinoma, adenocarcinoma, and large-cell carcinoma. Lung adenocarcinoma (LADC) is the main subtype, accounting for about 40% of all lung cancers [2]. It has mainly occurred in the terminal bronchioles and alveoli, which are not easily palpable by bronchoscopy. This brings more challenges to the diagnosis and treatment of LADC. Proto-oncogenes are known to play important roles in tumor formation, thus gaining insight into their regulation mechanism is helpful to develop effective therapies of lung adenocarcinoma.

The eukaryotic translation initiation factors (EIFs) play a critical role during eukaryotic translation. Among these, the eukaryotic translation initiation factor 3 (eIF3) family, which contains 13 subunits (eIF3a-eIF3m), is considered the largest (about 800 kDa) and most complex one [3]. EIF3 functions as a scaffold that promotes the binding between mRNA and 40S subunits and the assemble of 43S pre-initiation complex to control the protein synthesis in ribosomal [4]. Five of the core subunits of eIF3 (eIF3a, b, c, g, and i) are conserved in all eukaryotes, whereas the remaining subunits existed only in mammal [5]. Reports have shown that several eIF3 subunits are related to the occurrence of various cancer types, nevertheless, their roles and mechanisms in tumor progression are not the

same. EIF3a translational regulated the HIF-1α and promotes glycolysis of hepatocellular carcinoma [6]. EIF3b activated the PI3K/AKT/mTOR pathway and functions as an oncogenic protein in gastric cancer [7]. EIF3d stabilized GRK2 kinase and promoted the development of gallbladder cancer [8]. EIF3h protects YAP from ubiquitous degradation and facilitated invasion and metastasis of cancer cells [9]. EIF3i leads to the canceration of intestinal epithelial cells by regulating COX-2 protein synthesis [10]. EIF3m is the last identified EIF3s subunit, its role in lung adenocarcinoma has not yet been determined.

The purpose of the current study is to investigate the role of EIF3m in LADC and its mechanism. The analysis of public data shows that EIF3m is aberrantly up-regulated in LADC and the strong expression of EIF3m was prominently related to the poor prognosis. The functional investigations demonstrated the oncogenic activity of EIF3m *in vitro* and *in vivo*. Further, we discovered that EIF3m could bind to the 5'UTR of CAPRIN1 and promote its expression. CAPRIN1 was also proved to be a tumorigenic factor in the current work. Besides, the interaction between EIF3m and UCHL5 was confirmed, which stabilized EIF3m from ubiquitinated degradation. To sum up, we described a proto-oncogene axis of UCHL5/EIF3m/CAPRIN1 in LADC.

Materials and methods

Cell lines

The human bronchial epithelial cell line 16HBE and BEAS-2B were obtained from Procell (Wuhan, China) and maintained in RPMI-1640 medium (HyClone, Logan, UT, USA) supplemented with 10% fetal calf serum and 1%P/S. The lung adenocarcinoma cell lines A549, NCI-H1437, and NCI-H1395 were obtained from Procell. The lung adenocarcinoma cell line NCI-H1975 was purchased from (iCell Bioscience Inc, Shanghai, China). The A549 cells were cultured in Ham's F-12K medium (Procell) supplemented with 10% fetal calf serum 1%P/S. The NCI-H1437, NCI-H1395, and NCI-H1975 cells were cultured in RPMI-1640 medium (HyClone) supplemented with 10% FBS and 1%P/S. All cells were maintained at 37°C in a humidified atmosphere of 5% CO_2.

Quantitative real-time PCR (qRT-PCR)

Total RNA was extracted by using the TRIpure reagent (Bioteke, Beijing, China), the cDNA was generated using Super M-MLV (Bioteke). The mRNA expression level was detected using a 2×Power Taq PCR MasterMix kit (Bioteke) and SYBR Green (Sigma, MO, USA). The relative mRNA fold change was calculated by the $2^{-\Delta\Delta CT}$ method. The primers sequences are listed in Supplementary Table 1.

Immunoblotting

The cells or tissues lysates were prepared in RIPA buffer, then equal amounts of proteins were resolved by SDS-polyvinylidene difluoride gel. The proteins were then electrically transferred to the PVDF membranes. The primary antibodies used in the immunoblotting was as follows: EIF3m (1:1000, Thermo Scientific, Waltham, MA, USA), CAPRIN1 (1:1000, ABclonal, Wuhan, China), TRAF6 (1:1000, ABclonal), UCHL5 (1:200, Santa, Santa Cruz, CA, USA).

Plasmid construction and cell transfection

The coding sequences (CDS) of EIF3m, CAPRIN1, or UCHL5 were inserted into the NheI/BamHI sites of the pcDNA3.1 plasmid (Clontech, Palo Alto, CA, USA). The EIF3m shRNA sequences (shRNA1, target sequence: 5'-GGAACCAGACAAGCAAGAAGC-3'; shRNA2, target sequence: 5'-GCCATCCAGTACATCCCAACT-3'), CAPRIN1 shRNA sequences (target sequence: 5'-GGTGATCGACAAGAAACTTCG-3') or UCHL5 shRNA (target sequence: 5'-GCAAAGAAAGCTCAGGAAACC-3') sequences was respectively inserted into the BamHI/KpnI sites of pRNAH1.1 vector (Genscript, Nanjing, Jiangsu, China). Cell transfection was carried out by using the Lipofectamine 2000 kit according to the users' instructions (Invitrogen, CA, USA), and stably transfected cells were obtained by G418 screening.

Cell proliferation and colony formation assay

For CCK-8 cell proliferation assay, the cells were cultured in a 96-well plate at 3×10^3 cells/well, next, the CCK-8 working solution (Sigma, Louis, MO, USA) was added at the indicated time points. The absorbance at 450 nm was detected with a Microplate reader (ELx-800,

Biotek Instruments, VT, USA). To detect cell clone formation, the cells were seeded in a 60 mm plate at 200 cells/well density, the formatted colonies were detected on the 14th day by stained with 1% crystal violet.

Flow cytometry

The apoptosis detection kit (Beyotime, Haimen, China) was used to detect the apoptotic cells. In brief, the cells were incubated with FITC-conjugated Annexin V and propidium iodide in dark for 15 min. Then the cells were resuspended by using the binding buffer, at last, apoptotic cells were analyzed by flow cytometry (Aceabio, CA, USA).

Wound-healing assay

The transfected cells were plated in a 6-well culture dish and grown to 80% confluence, a straight scratch was made with a micropipettor tip, then the cells were cultured for another 24 h. Images were taken at the beginning and the end of the incubation. The cell migration distance was determined and normalized to that at 0 h.

Transwell assay

The transwell chamber (Corning, Tewksbury, MA, USA) pre-coated with matrigel matrix (BD, Ann Arbor, MI, USA) was employed to measure the cell invasion activity. The cells were seeded into the upper chambers at a density of 2×10^4/insert. The lower compartment was padding with complete medium containing 30% FBS. After 24 h of incubation, the cells on the bottom side of the chambers were fixed and stained with 0.5% crystal violet, and photographed under a microscope (BX53, Olympus, Tokyo, Japan).

Daul-luciferase reporter assay

The pGL4.10 vector (Promega Inc., Madison, WI, USA) containing the 141 bp CAPRIN1 5'-untranslated regions (5'-UTR) was co-transfected into the HEK293T cell with the EIF3m over-expression vector or co-transfected into the EIF3m-shRNA vector into the NCI-H1975 cells. Forty-eight hours later, the luciferase activities were determined by using the Dual-Luciferase Reporter Gene Assay Kit (Promega Inc., Madison, WI, USA) following the manufacturer's manual.

RNA immunoprecipitation (RIP)

The RIP assay was carried out by the EZ-Magna RIP kit (Millipore, Bedford, MA, USA) following the manufacturer's instructions. Cells were lysed with RIP buffer containing RNase inhibitor and protease inhibitor. Then the lysates were incubated with RIP buffer supplemented with magnetic beads conjugated to the EIF3m antibody (Abcam, Cambridge, MA, USA) at 4°C overnight. Next, the RNA-protein complex was incubated with proteinase K to isolate the coprecipitated RNA. After purification, the RNAs were analyzed by RT-PCR. The sequences of the primer were listed in Supplementary Table 1.

RNA-pull down assay

The RNA-pull-down experiment was performed by using the Pierce Magnetic RNA-protein Pull-Down Kit (Thermo, Waltham, MA, USA) following the manufacturer's protocol. In short, the 5'UTR sequence of CAPRIN1 was in vitro transcribed. Then the biotinylated RNA was mixed with cell extract and incubated with streptavidin-linked beads for 2 h at 25°C. The bead-RNA-protein complexes were washed 3 times and boiled in SDS buffer. At last, the retrieved protein was separated by SDS-polyvinylidene difluoride gel and the specific band was analyzed by western blot.

Co-immunoprecipitation and ubiquitination detection

The equal amounts of protein extracts were incubated with EIF3m antibody (Proteintech), UCHL5 antibody (Abcam), or control IgG at 4°C overnight. Thereafter, 60 µl protein A plus-agarose were added and incubated at 4°C for another 2 h. Afterward, the pellet was harvested by centrifugation and then washed with PBS for three times. The immunoprecipitate was then separated by SDS-polyvinylidene difluoride gel and detected by immuno-blotted with the UCHL5 antibody, EIF3m antibody, or HA-tag antibody.

Immunofluorescence

The cells were fixed with 4% paraformaldehyde and permeabilized with 0.1% triton X-100 for 30 min at 25°C. After incubated with 5% goat serum for 15 min, the cells were blotted with the rabbit anti-EIF3m antibody (1:100,

Proteintech) and mouse anti-UCHLF5 antibody (1:50, Santa) overnight at 4°C. After washing, the cells were stained with Cy3-conjugated goat anti-rabbit IgG (Beyotime, Haimen, China) or FITC-conjugated goat anti-mouse IgG (Beyotime), and the nuclei were counterstained with DAPI (Aladdin, Shanghai, China). The images were captured by a fluorescence microscope (BX53, Olympus, Tokyo, Japan).

In vivo experiments

All animal maintenance and handling were carried out following the Guide for the Care and Use of Laboratory Animals and approved by the Ethics Committee of the General Hospital of Northern Theater Command. The 5-6 weeks old BALB/c nude mice were obtained from HFK bioscience co., LTD (Beijing, China) with the License no. SCXK (Jing) 2019-0008. The mice were injected with 5×10^6 cells on the right flank subcutaneously. The tumor volume was detected once every 3 days when the tumor body was visible. On the 28th day after inoculation of the cell, the mice were sacrificed, then the xenograft tumors were collected. In metastasis assay, the mice were intravenously injected with 2×10^6 cells and allowed to develop lung metastases for 50 days. Then the lung tissues were collected for subsequent detection.

Pathological analysis

The tissues were fixed, embedded in paraffin, and sectioned into 5-μm thickness. The H&E staining were carried out according to the standard procedure as Jia et al. reported [11]. For immunohistochemical detection, the sections were incubated with goat serum, then immuneblotted with the Ki67 antibody (1: 100, Abclonal) overnight at 4°C. After staining with the HRP-conjugated goat anti-rabbit secondary antibody, the slices were counterstained with hematoxylin. The apoptotic cells of the tumor tissues were detected by the TdT-mediated dUTP Nick-End Labeling (TUNEL) assay kit (Roche, Penzberg, Germany) according to the user's manual.

Online analysis of the TCGA datasets

The public datasets from TCGA were analyzed by online tools. The EIF3m expression and overall survival in lung adenocarcinoma were analyzed by using the UALCAN (http://ualcan.path.uab.edu/index.html) with expression profile or Kaplan-Meier plots. The correlation between two genes in lung adenocarcinoma was analyzed by using the GEPIA (http://gepia.cancer-pku.cn/index.html).

Statistical analysis

The experimental data were presented as the mean ± SD. Statistical analysis was conducted using Graphpad Prism version 8.0 (Graphpad, San Diego, CA, USA). The difference between two groups was analyzed using Student's t-test, and the difference between three or more groups was analyzed using one-way ANOVA. The survival probability was analyzed using Kaplan-Meier by the log-rank test. The correlation analysis was carried out with the Pearson correlation coefficient. $P<0.05$ was regarded as a statistical difference.

Results

EIF3m is aberrantly high expressed in LADC tissues and predicts poor prognosis

We queried the public datasets from TCGA to identify the expression of EIF3m in LADC samples. The data showed that the amounts of transcripts of EIF3m were significantly higher in LADC tumors (**Figure 1A**). Kaplan-Meier analysis results indicate that the higher EIF3m level was positively correlated with a lower survival probability of LADC patients (**Figure 1B**). The correlation between EIF3m and clinicopathological features was further analyzed, as shown in **Figure 1C** and **1D**, the high EIF3m level was also associated with the cancer stages and nodal metastasis status of LADC. Further, we detected the expression of the EIF3m protein level in normal bronchial epithelial cell lines and LADC cells. The results revealing that the protein level of EIF3m was obviously overexpressed in LADC cells than in normal bronchial epithelial cells (**Figure 1E**). These results indicate that EIF3m may associate with the progression of LADC.

EIF3m promoted LADC growth in vitro and in vivo

We employed gain-and loss-of-function assays to investigate the biological function of EIF3m in LADC. Considering the endogenous expression of EIF3m showed in **Figure 1E**, we devel-

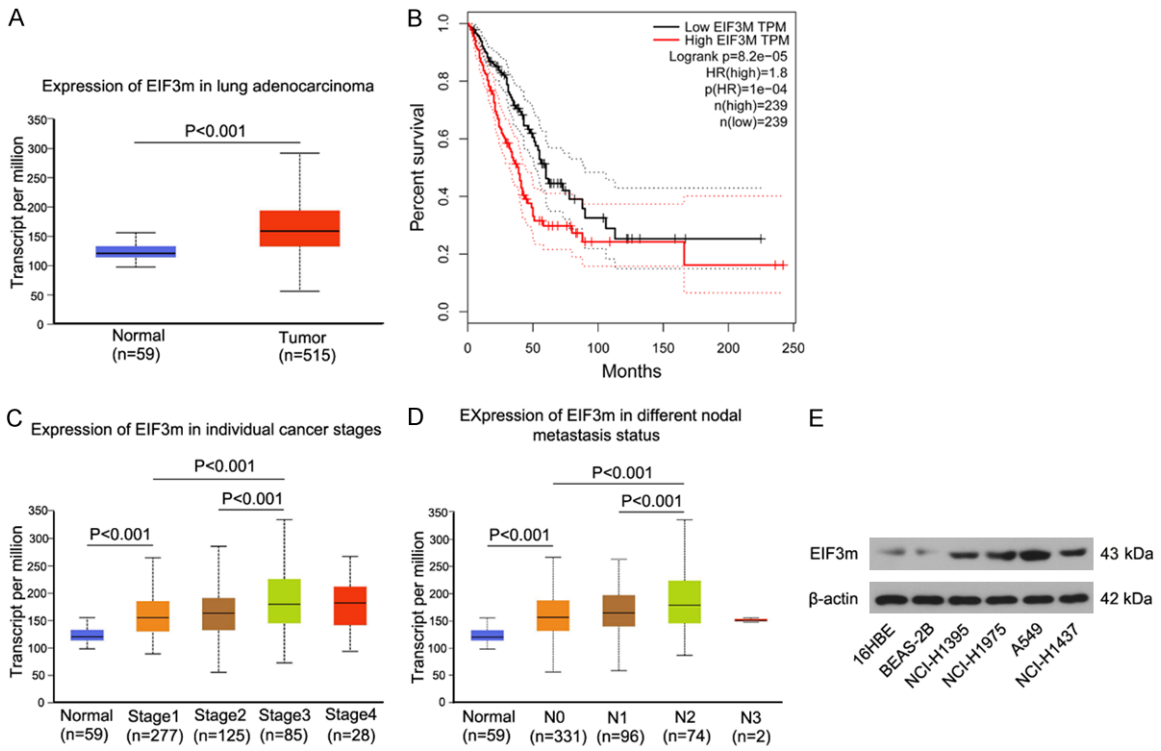

Figure 1. EIF3m expression is increased in LADC tissues and the high level of EIF3m is associated with malignant phenotypes and poor clinical outcomes in LADC patients. Analysis of the expression of EIF3m from the TCGA database. The expression of EIF3m in normal and LADC tumor tissues (A), the overall survival (B), the expression of EIF3m in individual cancer stages (C), and the expression of EIF3m in different nodal metastasis status (D). The expression of EIF3m in normal airway epithelium cell lines and LADC cell lines was determined by western blot (E). The data are expressed as the mean mean ± SD.

oped NCI-H1975 and NCI-H1395 cells that stably silenced or over-expressed EIF3m. The level of EIF3m in these cells was confirmed by western blot (**Figures 2A** and **3A**). The CCK-8 and colony formation results exhibited that the up-regulation of EIF3m dramatically enhanced the proliferation and colony formation activities of these LADC cells (**Figure 2B** and **2C**), however, cell proliferation activity and colony formation capacity was significantly inhibited by the knockdown of EIF3m (**Figure 3B** and **3C**). At the same time, knockdown of EIF3m also induced apoptosis of LADC cells (**Figure 3D**).

In order to demonstrate the effects of EIF3m on LADC growth in vivo, we established a xenograft model in nude mice. We found that the tumor growth evidently faster in EIF3m over-expression group than that in the vector group (**Figure 2D**). In the opposite, the tumor growth was suppressed in the EIF3m knockdown group when compared to the negative control group (**Figure 3E**). Immunohistochemical staining revealed that the proliferating cells (Ki67 positive) were reduced and the apoptotic cells (TUNEL positive) were increased by the down-regulation of EIF3m (**Figure 3F**). The expression of EIF3m in these tumor tissues was examined by western blot, as expected, the EIF3m level was increased in EIF3m over-expression group and reduced in EIF3m down-regulated group (Supplementary Figure 1A and 1B). Collectively, our results suggest that EIF3m promotes the proliferation and growth of LADC *in vitro* and *in vivo*.

EIF3m promoted invasion and metastasis of LADC

To explore the effects of EIF3m on the migration and invasion potential of LADC cells, the wound healing and transwell invasion assays were further performed. The results exhibited that forced expression of EIF3m markedly enhanced the migration and invasion activities of LADC cells (**Figure 4A** and **4B**), however,

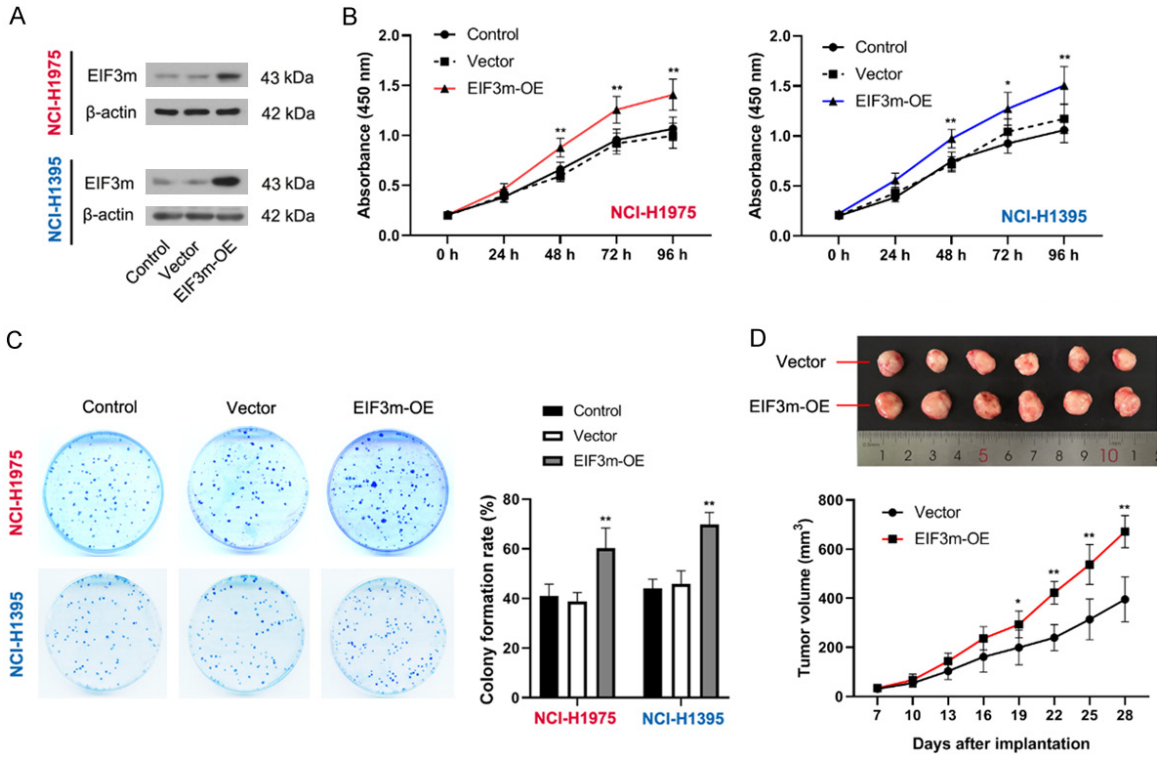

Figure 2. Over-expression of EIF3m promoted the proliferation of LADC cells *in vitro* and *in vivo*. EIF3m was stably over-expressed in NCI-H1975 and NCI-1395 cells, the expression of EIF3m was determined by western blot (A). Cell proliferation was detected by CCK-8 assay (B), the colony formation activity was measured by colony formation assay, and the ratio of clone formation number to seeded cell number was recorded as the colony formation rate (C). The cells were subcutaneously injected into the mice and the tumor volume was measured every 3 days (D). The data are expressed as the mean mean ± SD. *P<0.05, **P<0.01 *vs.* vector-transfected cells.

these activities were significantly suppressed by the knockdown of EIF3m (**Figure 5A** and **5B**). Also, the roles of EIF3m in metastasis of LADC cells were determined in vivo. As shown in **Figure 4C**, the up-regulation of EIF3m in LADC cells resulted in extensive metastatic nodules in the lung. In contrast, down-regulation of EIF3m in LADC cells exhibited reduced metastatic nodules when compared to the NC group (**Figure 5C**). The H&E staining results of the lung tissues demonstrated that the number of metastatic foci and size of lung metastases was obviously increased by the over-expressed of EIF3m (**Figure 4D**), and reduced by the knockdown of EIF3m (**Figure 5D**). These results indicate that EIF3m promoted the invasion and metastasis of LADC.

EIF3m bind to the 5'UTR of CAPRIN1 and promoted its expression

Studies have suggested that EIF3 could regulate the expression of several oncogenes [3, 12], thus, the mRNA level of these factors was detected to reveal the mechanism on how EIF3m implicated in the development of LADC. The results from real-time PCR displayed that the expression of TRAF6, CAPRIN1, NUP160, and PDHX were distinctly related to the EIF3m level (**Figure 6A** and **6B**). Considering that the EIF3 subunits could bind to the 5'UTR of specific transcripts [3], we further employed RIP assay to exam whether EIF3m affects these candidate mRNAs by the same mechanisms. The results showed that after immunoprecipitation with EIF3m, only the 5'UTR primers of CAPRIN1 amplified positive products (**Figure 6C**). To further identify the interaction between CAPRIN1 and EIF3m, we pulled down CAPRIN1-5'UTR-binding proteins using an RNA pull-down assay and the results displayed that EIF3m was a CAPRIN1-associated protein (**Figure 6D**). The binding of EIF3m to CAPRIN1 was further confirmed by immune-blot in RNA pull-down retrieved proteins (**Figure 6E**). These results

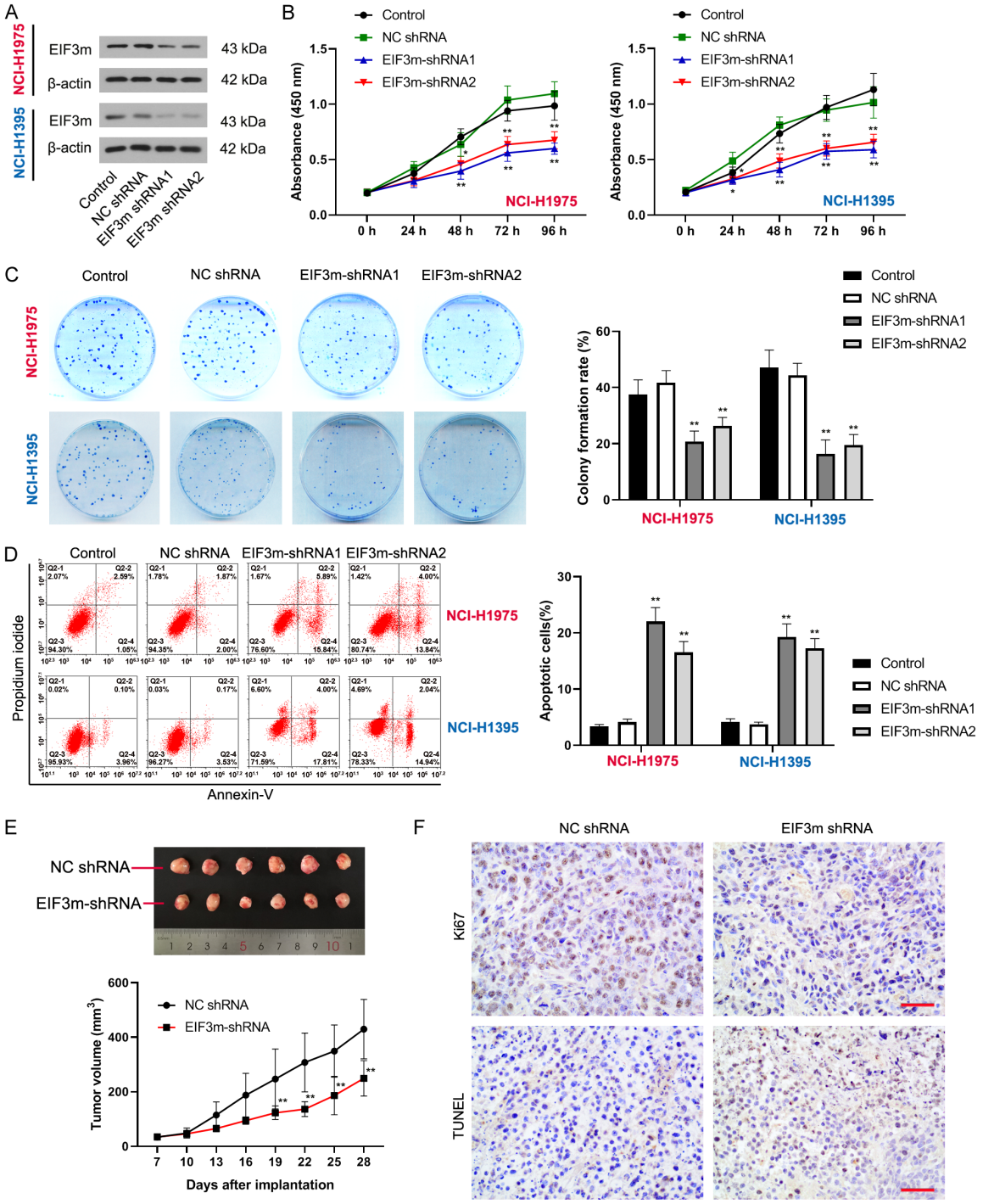

Figure 3. Down-regulation of EIF3m suppressed the proliferation and induced apoptosis of LADC cells *in vitro* and *in vivo*. EIF3m was stably downregulated in NCI-H1975 and NCI-1395 cells, the expression of EIF3m was determined by western blot (A). Cell proliferation was detected by CCK-8 assay (B), the colony formation activity was measured by colony formation assay, and the ratio of clone formation number to seeded cell number was recorded as the colony formation rate (C), the apoptotic cells were measured by flow cytometry and the percentage was displayed (D). The cells were subcutaneously injected into the mice and the tumor volume was measured every 3 days (E). The immunohistochemical staining of Ki67 and TUNEL in tumor tissues (F), scale bar, 50 μm. The data are expressed as the mean mean ± SD. *P<0.05, **P<0.01 *vs.* NC shRNA transfected cells.

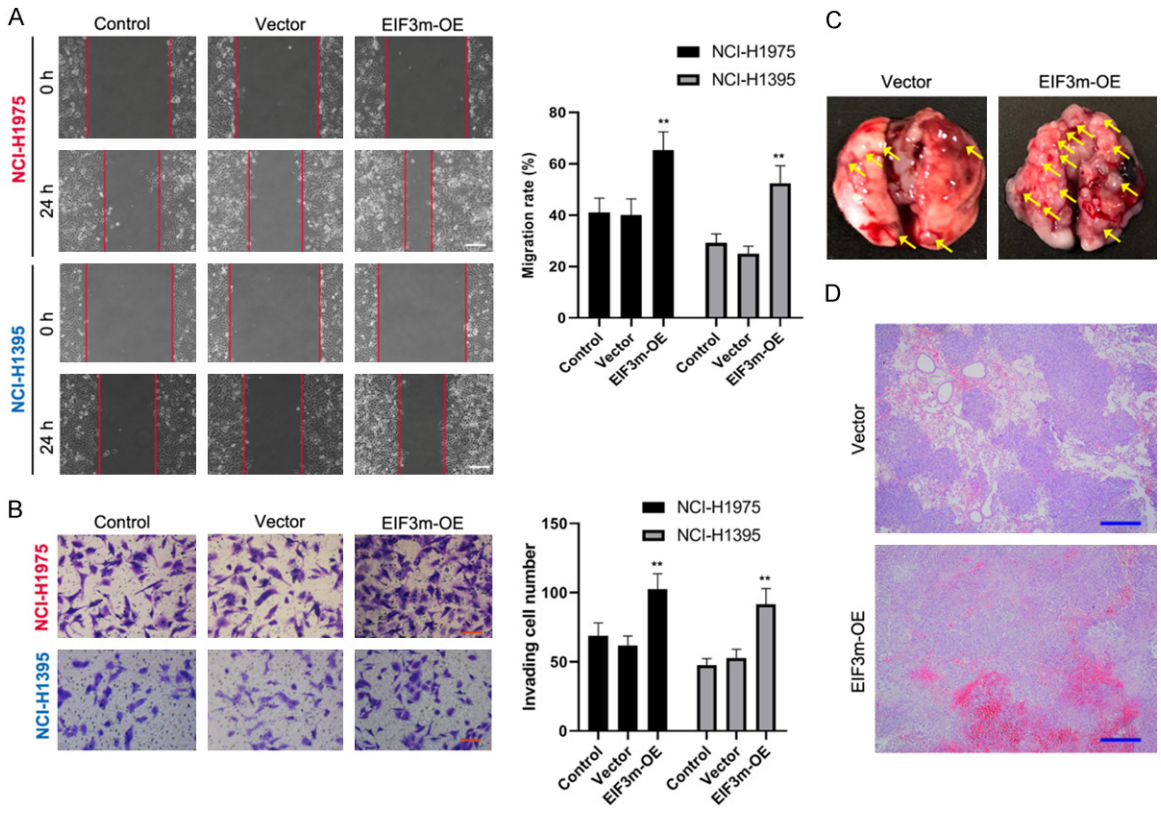

Figure 4. Over-expression of EIF3m promoted the migration and invasion of LADC cells *in vitro* and *in vivo*. The migration activity was measured by wound-healing assay and the migration rate was calculated (A), scale bar, 200 μm; the invasion potential was detected by transwell assay and the invading cell number was counted (B), scale bar, 100 μm. The NCI-H1975 cells were intravenously injected into the mice, the lung metastases were observed 50 days after the injection (C), and the lungs were stained by H&E (D), scale bar, 500 μm. The data are expressed as the mean mean ± SD, **P<0.01 *vs.* vector-transfected cells.

indicated that EIF3m directly binding to the 5'UTR of CAPRIN1.

To validate whether EIF3m act as a positive or negative regulator of CAPRIN1, we performed the dual-luciferase reporter assay. The HEK-293T cells transfected with pGL4.10-CAPRIN1-5'UTR exhibited increased luciferase activity, co-transfected the cells with EIF3m-over-expression vector and pGL4.10-CAPRIN1-5'UTR further up-regulated the luciferase activity (**Figure 6F**). The luciferase activity of NCI-H1975 cells transfected with pGL4.10-CAPRIN1-5'UTR was significantly up-regulated, however, these effects were strongly inhibited by the EIF3m shRNA (**Figure 6G**). These results suggesting that endogenous or exogenous EIF3m all promoted the stability of the CAPRIN1 mRNA. The results from western blot also proved that over-expression of EIF3m increased CARPIN1 protein level, whereas, knockdown of EIF3m reduced the CARPIN1 protein level (**Figure 6H**). Besides, the TCGA database showed a positive correlation between EIF3m and CAPRIN1 (**Figure 6I**).

EIF3m promoted proliferation, invasion, and suppressed apoptosis of LADC cells via CAPRIN1

To verify the hypothesis that EIF3m affects the malignant phenotype of LADC cells through CAPRIN1, we knockdown or up-regulated the CAPRIN1 in EIF3m over-expression or down-regulation cells. The efficiency of the knock-down or over-expression of CAPRIN1 was verified by western blot (Supplementary Figure 1C and 1D). We found that EIF3m induced proliferation and invasion of LADC cells were rescued by the down-regulation of CAPRIN1 (**Figure 7A** and **7B**). At the same time, the loss of EIF-3m induced apoptosis of LADC cells was also counteracted by the up-regulation of CAPRIN1 (**Figure 7C**). These findings revealed that

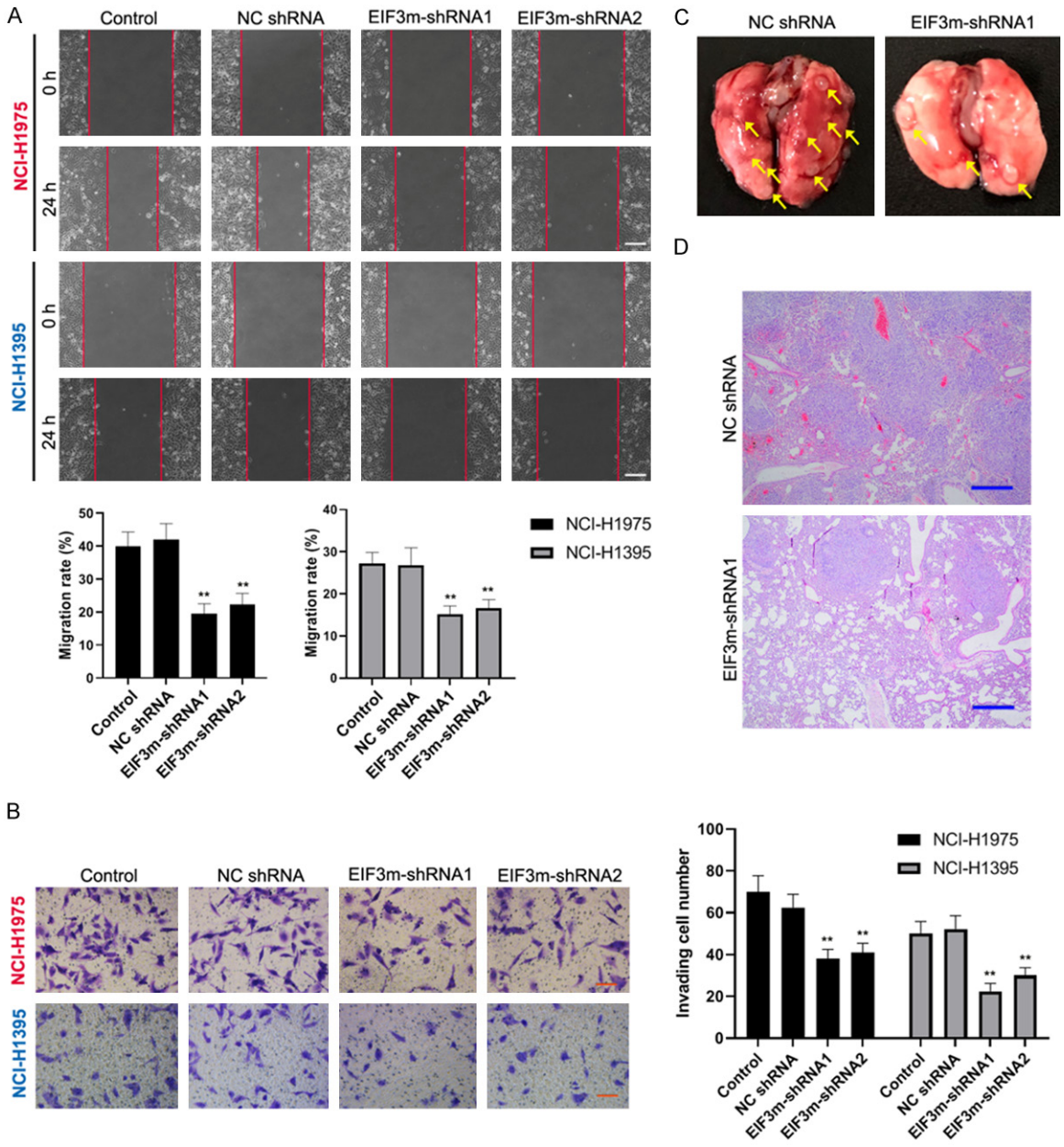

Figure 5. The knockdown of EIF3m suppressed the migration and invasion of LADC cells *in vitro* and *in vivo*. The migration activity was measured by wound-healing assay and the migration rate was calculated (A), scale bar, 200 μm; the invasion potential was detected by transwell assay and the invading cell number was counted (B), scale bar, 100 μm. The NCI-H1975 cells were intravenously injected into the mice, the lung metastases were observed 50 days after the injection (C), and the lungs were stained by H&E (D), scale bar, 500 μm. The data are expressed as the mean mean ± SD, **P<0.01 *vs.* NC shRNA transfected cells.

CAPRIN1 is necessary for the carcinogenicity activity of EIF3m.

UCHL5 interacted with EIF3m in LADC cells

To reveal the reasons for the high expression of EIF3m in LADC, we analyzed several molecules implicated in protein degradation and found that EIF3m interacted with the deubiquitinase UCHL5 through co-immunoprecipitation and western blot assay (**Figure 8A**). The gain- and loss-of-function of UCHL4 assays were employed to further detect whether UCHL5 affects the expressions of EIF3m and CAPRIN1. As shown in **Figure 8B**, forced overexpression of UCHL5 up-regulated EIF3m and CAPRIN1 pro-

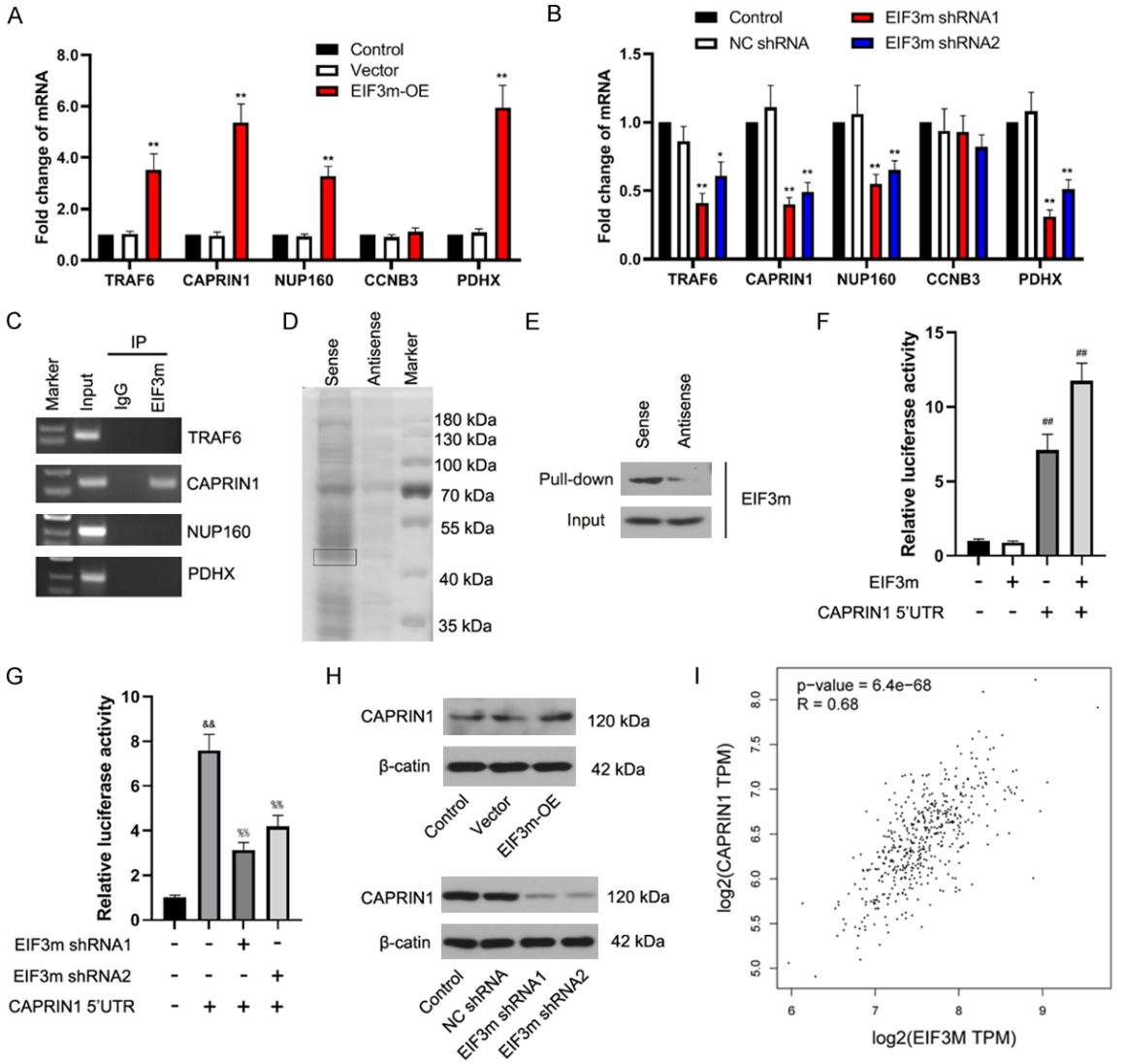

Figure 6. EIF3m bind to the 5'UTR of CAPRIN1 and positively regulate its expression. The expression of the candidate genes in NCI-H1975 was examined by qRT-PCR (A & B). The binding of EIF3m on the 5'UTR of candidate genes was detected by the RNA immunoprecipitation (RIP) assay (C). The CAPRIN1 5'UTR binding proteins were detected by SDS-polyvinylidene difluoride gel (D), the frame indicates EIF3m, and the specific association of EIF3m and CAPRIN1 was determined by western blot (E). The regulation of EIF3m on the translation activity of CAPRIN1 was verified by the dual-luciferase reporter assay in HEK293T cells (F) and NCI-H1975 cells (G). The expression of CAPRIN1 was detected by western blot (H). The correlation between EIF3m and CAPRIN1 from the TCGA database was analyzed (I). The data are expressed as the mean ± SD, *P<0.05, **P<0.01 *vs.* Vector or NC shRNA transfected cells, ##P<0.01 *vs.* EIF3m-OE transfected cells, &&P<0.01 *vs.* control cells and %%P<0.01 *vs.* CAPRIN1 5'UTR transfected cells.

tein level, on the other hand, knock-down of UCHL5 resulted in the reduction of EIF3m and CARPIN1 levels. Further, the immunofluorescence assay not only confirmed the expression changes of EIF3m induced by UCHL5 but also verified the overlapping signals between EIF3m and UCHL5 (**Figure 8C**). Overall, these results indicate the interaction between UCHL5 and EIF3m.

UCHL5 stabilized EIF3m at protein level

A previous study has suggested the de-ubiquitinating role of UCHL5 in lung fibroblasts [13], this prompted us to explore whether the interaction between UCHL5 and EIF3m cloud stabilizes the EIF3m protein. The cells were transfected with UCHL5-overexpression vector or specific UCHL5 shRNA and treated with cyclo-

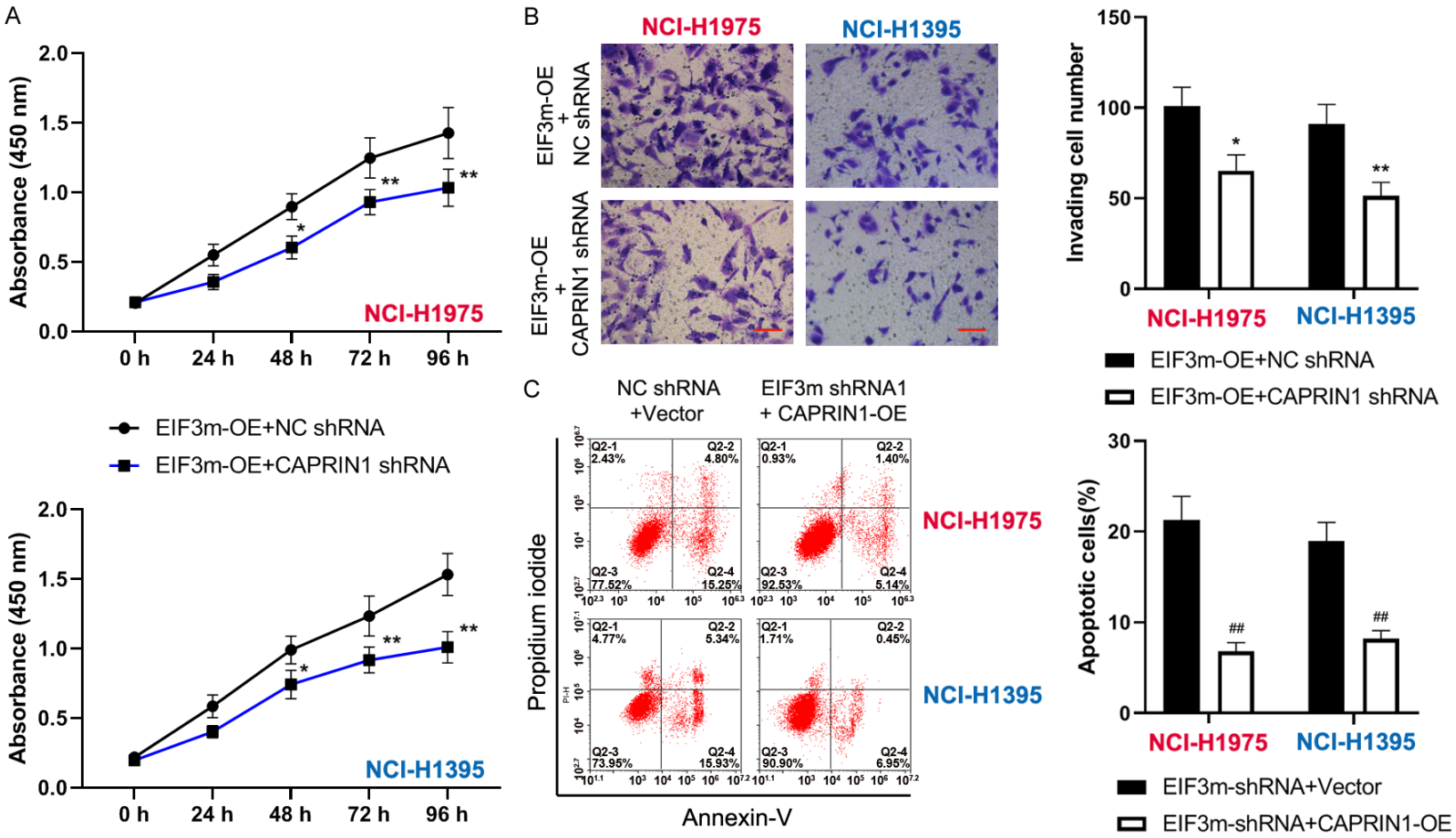

Figure 7. EIF3m induced malignant phenotype of LADC cells was mediated by CAPRIN1. Cell proliferation was examined by CCK-8 assay (A), cell invasion activity was detected by transwell assay, and the invading cell number was counted (B), scale bar, 100 μm; cell apoptosis was measured by flow cytometry and the percentage of apoptotic cells was displayed (C). The data are expressed as the mean mean ± SD, *P<0.05, **P<0.01 *vs.* EIF3m-OE + NC shRNA group, ##P<0.01 *vs.* EIF3m-shRNA + Vector group.

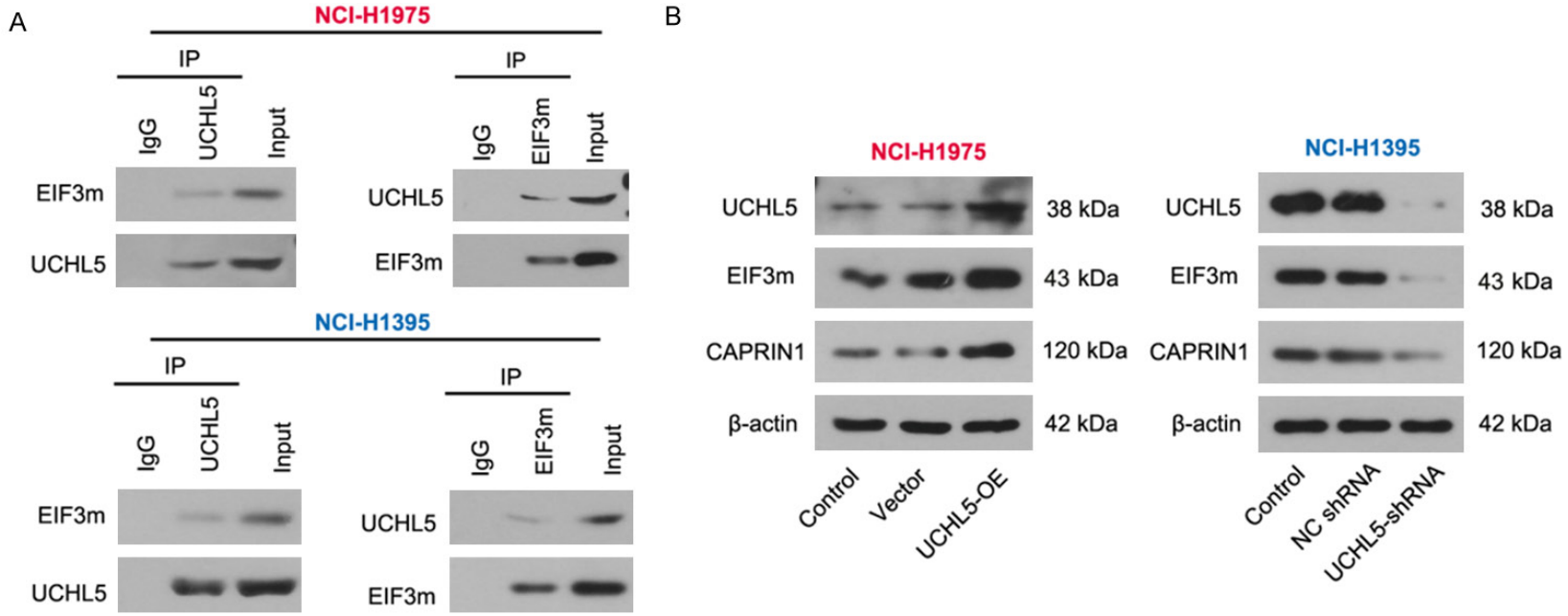
A
NCI-H1975
IP
IgG
UCHL5
Input
EIF3m
UCHL5
IP
IgG
EIF3m
Input
UCHL5
EIF3m
NCI-H1395
IP
IgG
UCHL5
Input
EIF3m
UCHL5
IP
IgG
EIF3m
Input
UCHL5
EIF3m
B
NCI-H1975
UCHL5
38 kDa
EIF3m
43 kDa
CAPRIN1
120 kDa
β-actin
42 kDa
Control
Vector
UCHL5-OE
NCI-H1395
UCHL5
38 kDa
EIF3m
43 kDa
CAPRIN1
120 kDa
β-actin
42 kDa
Control
NC shRNA
UCHL5-shRNA

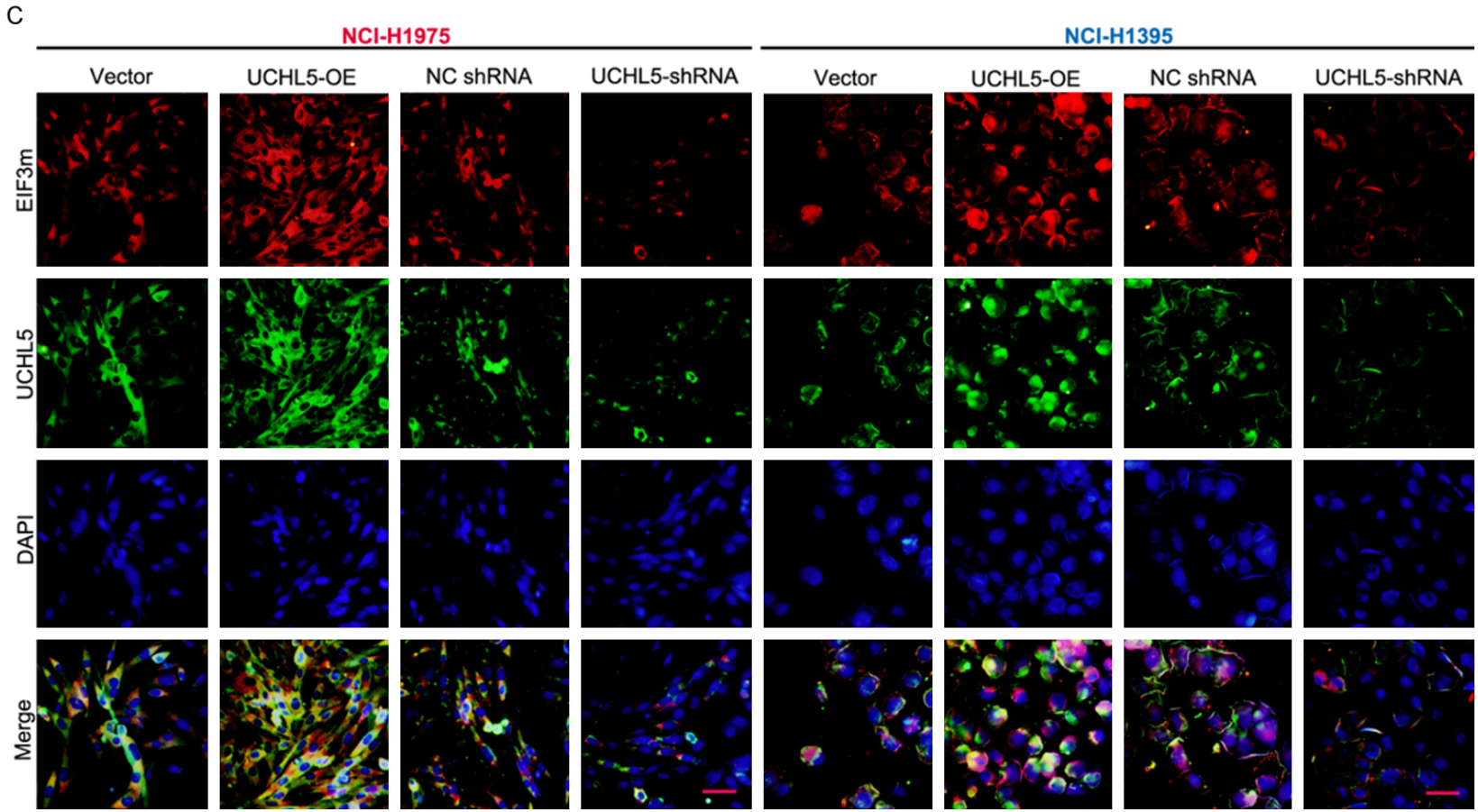

Figure 8. EIF3m interacted with UCHL5. The co-immunoprecipitation assay was employed to detect the interaction between EIF3m and UCHL5 (A). The expression of EIF3m, UCHL5, and CAPRIN1 was measured by western blot (B), the expression of EIF3m and UCHL5 was evaluated by Immunofluorescence (C), scale bar, 50 μm.

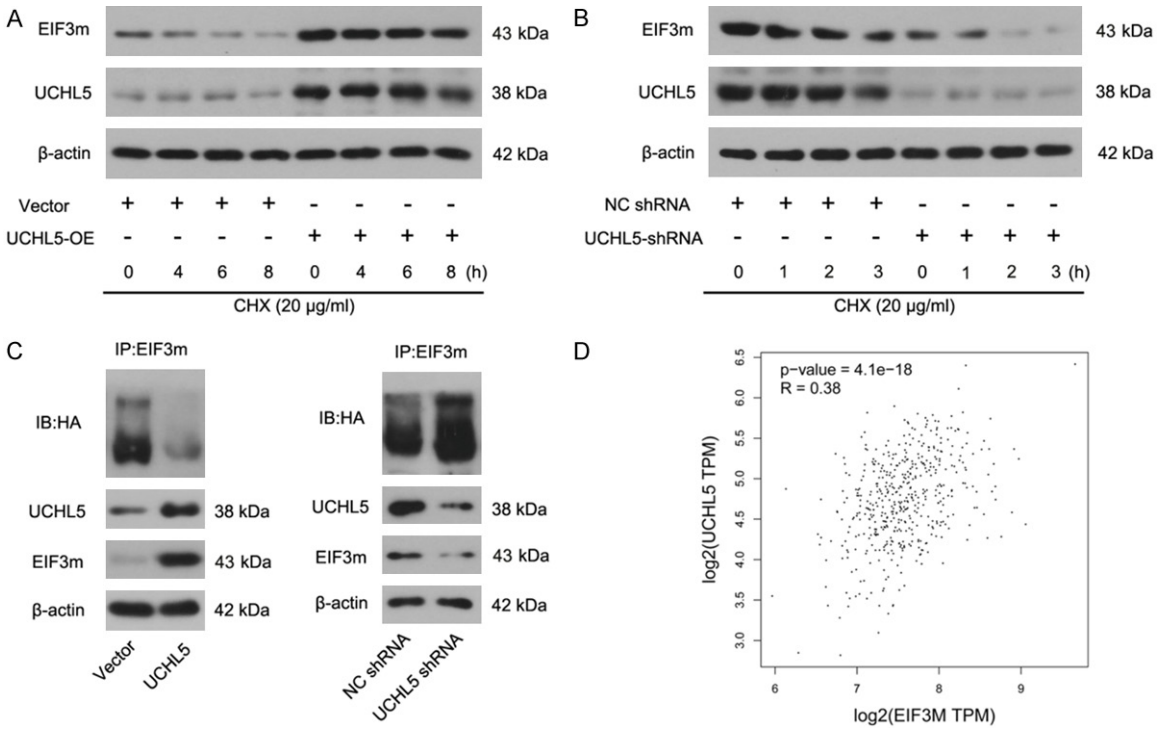

Figure 9. UCHL5 stabilized EIF3m. The NCI-H1975 cells were treated with cycloheximide (CHX) for the indicated time, the expression of EIF3m and UCHL5 was determined western blot (A & B). The cells were transfected with HA-tagged ubiquitin vector and pretreated with 10 μg proteasome inhibitor MG-132 for 6 h, then the ubiquitination status was examined by co-immunoprecipitation (C). The correlation between EIF3m and UCHL5 from the TCGA database was analyzed (D).

heximide (CHX) for different times, then the expression of EIF3m and UCHL5 was determined. It was shown that the degradation of EIF3m was suppressed by UCHL5 overexpression, and promoted by UCHL5 knockdown (**Figure 9A** and **9B**). To determine whether UCHL5 stabilize EIF3m dependent on its deubiquitinating activity, the cells were transfected with HA-tagged ubiquitin vector and pretreated with 10 μg proteasome inhibitor MG-132 for 6 h, then the ubiquitination status was examined. The results showed that overexpression of UCHL5 weakened the ubiquitination of EIF3m, while UCHL5 down-regulation strengthened the ubiquitination of EIF3m (**Figure 9C**). Further TGCA database analysis exhibited that the level of EIF3m was positively correlated with UCHL5 (**Figure 9D**), and the expression of UCHL5 was also significantly upregulated in LADC (Supplementary Figure 2C). These data suggested that UCHL5 functioned as a deubiquitinase to inhibit the degradation of EIF3m.

UCHL5 affects EIF3m induced malignant phenotype of LADC cells

To further clarify the effects of UCHL5 in EIF3m induced malignant properties of LADC, the EIF3m over-expression cells were transfected with UCHL5 shRNA. The results of CCK-8 assay indicated that EIF3m-induced cell proliferation was significantly restrained by the down-regulation of UCHL5 (**Figure 10A**). The knock-down of UCHL5 also blocked the colony formation activity of EIF3m over-expressed cells (**Figure 10B**). The results from the transwell assay demonstrated that the raised invasion potential of EIF3m-overexpressing cells was declined by the inhibition of UCHL5 (**Figure 10C**). Combined with the effect of UCHL5 on EIF3m expression, these data suggest that UCHL5 could facilitate EIF3m induced proliferation and metastasis of LADC.

Discussion

The current work described the oncogenic potential of EIF3m in LADC and extended the

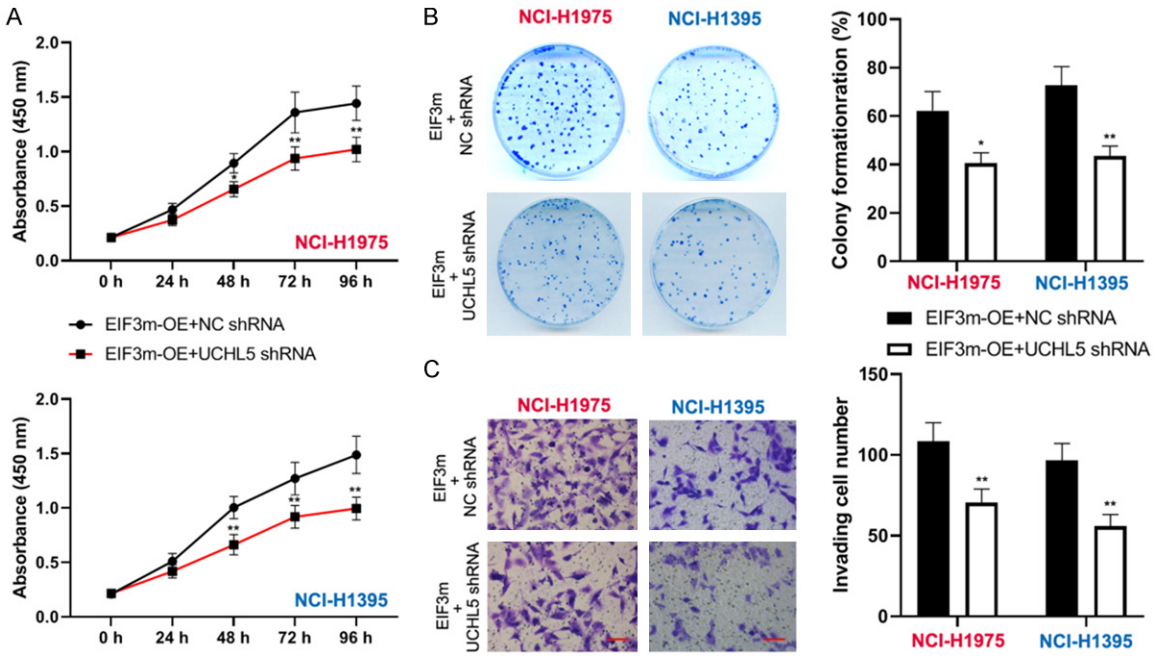

Figure 10. UCHL5 facilitates EIF3m induced malignant phenotype of LADC cells. Cell proliferation and colony formation were examined by CCK-8 assay (A) and colony formation assay and the ratio of clone formation number to seeded cell number was recorded as the colony formation rate (B), cell invasion activity was detected by transwell assay and the invading cell number was counted (C), scale bar, 100 μm. The data are expressed as the mean mean ± SD, *P<0.05, **P<0.01 *vs*. EIF3m-OE + NC shRNA group.

knowledge about EIF3m in tumor progression. Firstly, we revealed that EIF3m was highly expressed in LADC tissue and cell lines, the up-regulation of EIF3m indicated poor prognosis of LADC. Secondly, our *in vitro* and *in vivo* results proved that forced over-expression of EIF3m exacerbate the proliferation, neoplasia, and metastasis of LADC, while knockdown of EIF3m repressed these malignant behaviors. Thirdly, we explained the mechanism of how EIF3m promotes the development of LADC. EIF3m activated the expression of the oncogene CAPRIN1 at post-transcription level through directly binding to its 5'UTR. Finally, we elucidated that the interaction between UCHL5 and EIF3m stabilized the EIF3m protein from ubiquitin-mediated degradation, which also explained the reason for the abnormal over-expression of EIF3m in LADC. The current work unveiled that the UCHL5/EIF3m/CAPRIN1 axis promoted the tumorigenesis of LADC (**Figure 11**).

The translation initiation factor eIF3 complex was originally thought to be a kind of housekeeping initiation factor, in recent years, accumulating evidence indicates the other functions of eIF3m outside its general role. Divers studies linked eIF3 subunits to the development of cancers, including eIF3a, b, c, h [8, 14-16]. As the latest proved subunits, the function of eIF3m has rarely been explored. The studies in triple-negative breast cancer and colon cancer suggested that eIF3m could regulate several tumorigenesis-related genes and contribute to the tumorigenesis [12, 17]. Analogous to these studies, the pro-tumorigenic activity of eIF3m was further identified in LADC.

The disordered expression of tumor-related gene is a common hallmark of the etiology of cancer. The ribonomics approach in EIF3m silenced colon cancer cells identified the changes in the mRNA level of a subset of oncogenic genes [17]. Besides, the up-regulation of EIF3m elevated the mRNA level of oncogenes related to tumor growth in triple-negative breast cancer cells [12]. Thus, we postulated that EIF3m may also influence the expression of these oncogenic genes in LADC. In the current study, gain- and loss-of-function of EIF3m induced expression changes of these oncogenic genes in LADC cells was not completely consistent with that in other cancer tumors. Thus, the cancer-promoting mechanism of EIF3m may be divergent in different cancer types.

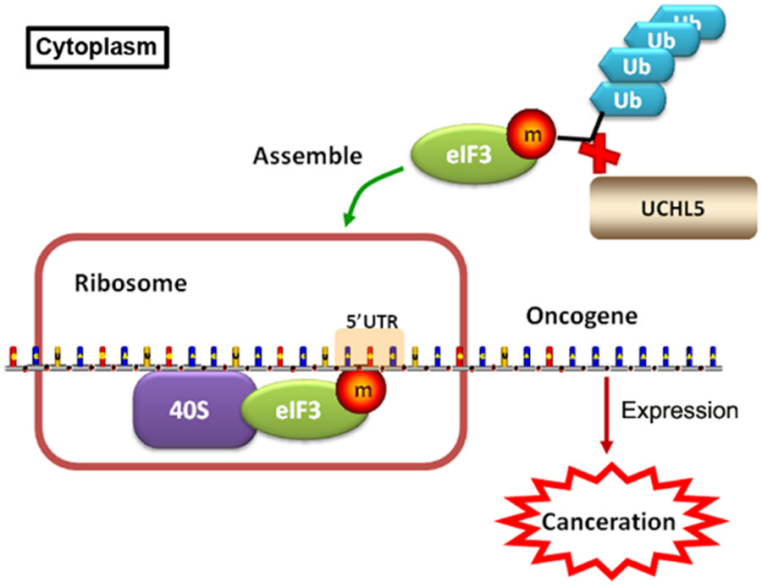

Figure 11. Proposed mechanism of the UCHL5/EIF3m/CAPRIN1 axis in the progression of LADC.

A 4-thiouridine photoactivatable ribonucleoside-enhanced crosslinking and immunoprecipitation (PAR-CLIP) assay has found that the EIF3a, b, d, and g could activate or repress the translation of specific genes by binding to their 5'UTR [3]. Therefore, we performed a RIP assay to identify the interaction between EIF3m and the 5'UTR of these candidate genes. The 5'UTR primers of TRAF6, NUP160, and PDHX didn't achieve positive products, except for CAPRIN1. The 5'UTR of mRNAs is one of the recognition elements of ribosomes and is known to be the mediator of translation initiation [18]. The other subunits of EIF3 such as EIF3a, EIF3i, EIF3h, all been showed to exacerbate oncogenesis by enhanced the translation of a large subset of oncogenic mRNAs [6, 7, 16]. Considering that the protein level of CARPIN1 was also affected by the modulation of EIF3m, we speculate that EIF3m activated the translation of CARPIN1. In addition to directly affecting the initiation of translation, the 5'UTR is also the pivotal region that affects the stability of mRNA [19], thus, EIF3m may stabilize the CAPRIN1 mRNA by the 5'UTR specific binding. It is also the reason why EIF3m affects the mRNA level of CAPRIN1.

Several studies indicate that CAPRIN1 is aberrantly up-regulated and is associated with poor prognosis in diverse tumor types [20-22]. However, its role in LADC has not been reported exactly. We analyzed the TCGA database and the data suggested that the expression of CAPRIN1 was prominently increased in LADC, and the high level of CAPRIN1 is correlated to the low survival rate of LADC (Supplementary Figure 2A and 2B). More importantly, EIF3m induced proliferation, invasion, and anti-apoptotic activities were markedly counteracted by the rescue of CAPRIN1. These findings indicate that CAPRIN1 functions as a cancer-promoting gene, and is essential in EIF3m induced malignancy in LADC.

The deubiquitinase UCHL5 was recognized as a component of the proteasome, that implicated in the regulation of multiple cellular processes [23], including the proliferation, apoptosis, and invasion of tumor cells [24-26]. The overexpression of UCHL5 de-ubiquitinated and stabilized the smad2/smad3 signal and contribute to the pathogenesis of idiopathic pulmonary fibrosis [13]. Our results proved that EIF3m could interact with the deubiquitinase UCHL5, and this interaction stabilized EIF3m from ubiquitin-induced degradation. The data from TCGA showed that UCHL5 is significantly up-regulated in LADC, and the high level of UCHL5 is strongly associated with the low survival percent (Supplementary Figure 2C and 2D). These may explain the reason why EIF3m is highly expressed in LADC tissues.

In summary, the present study demonstrated that EIF3m is highly expressed in LADC tissue and cell lines, the high level of EIF3m indicates the poor prognosis of LADC. EIF3m function as a proto-oncogene in LADC, these effects were partly mediated by the up-regulation of CAPRIN1. EIF3m seems to modulate the expression of CAPRIN1 by direct binding on its 5'UTR. Further, UCHL5 interacted with EIF3m and stabilized EIF3m from ubiquitin-related degradation. These findings suggest that the UCHL5/EIF3m/CAPRIN1 axis may be a potential target for the therapy of LADC.

Acknowledgements

This research was supported by grants from the Natural Science Foundation of Liaoning

Province (No. 20170540931 and No. 2019-MS-356).

Disclosure of conflict of interest

None.

Address correspondence to: Dr. Ruonan Chai, Department of Respiratory Medicine, The General Hospital of Northern Theater Command, 83 Wenhua Road, Shenyang 110016, People's Republic of China. Tel: +86-24-28851496; E-mail: lilypad_ff@126.com

References

[1] McGuire S. World Cancer Report 2014. Geneva, Switzerland: World Health Organization, International Agency for Research on Cancer, WHO Press, 2015. Adv Nutr 2016; 7: 418-419.
[2] Denisenko TV, Budkevich IN and Zhivotovsky B. Cell death-based treatment of lung adenocarcinoma. Cell Death Dis 2018; 9: 117.
[3] Lee AS, Kranzusch PJ and Cate JH. eIF3 targets cell-proliferation messenger RNAs for translational activation or repression. Nature 2015; 522: 111-114.
[4] Silvera D, Formenti SC and Schneider RJ. Translational control in cancer. Nat Rev Cancer 2010; 10: 254-266.
[5] Cate JH. Human eIF3: from 'blobology' to biological insight. Philos Trans R Soc Lond B Biol Sci 2017; 372: 20160176.
[6] Miao B, Wei C, Qiao Z, Han W, Chai X, Lu J, Gao C, Dong R, Gao D, Huang C, Ke A, Zhou J, Fan J, Shi G, Lan F and Cai J. eIF3a mediates HIF1alpha-dependent glycolytic metabolism in hepatocellular carcinoma cells through translational regulation. Am J Cancer Res 2019; 9: 1079-1090.
[7] Qi J, Dong Z, Liu J and Zhang JT. EIF3i promotes colon oncogenesis by regulating COX-2 protein synthesis and beta-catenin activation. Oncogene 2014; 33: 4156-4163.
[8] Liu T, Wei Q, Jin J, Luo Q, Liu Y, Yang Y, Cheng C, Li L, Pi J, Si Y, Xiao H, Rao S, Wang F, Yu J, Zou D and Yi P. The m6A reader YTHDF1 promotes ovarian cancer progression via augmenting EIF3C translation. Nucleic Acids Res 2020; 48: 3816-3831.
[9] Zhou Z, Zhou H, Ponzoni L, Luo A, Zhu R, He M, Huang Y, Guan KL, Bahar I, Liu Z and Wan Y. EIF3H orchestrates hippo pathway-mediated oncogenesis via catalytic control of YAP stability. Cancer Res 2020; 80: 2550-2563.
[10] Morris C, Tomimatsu N, Burma S and Jalinot P. INT6/EIF3E controls the RNF8-dependent ubiquitylation pathway and facilitates DNA double-strand break repair in human cells. Cancer Res 2016; 76: 6054-6065.
[11] Jia Y, Zhao S, Jiang T, Li X, Zhao C, Liu Y, Han R, Qiao M, Liu S, Su C, Ren S and Zhou C. Impact of EGFR-TKIs combined with PD-L1 antibody on the lung tissue of EGFR-driven tumor-bearing mice. Lung Cancer 2019; 137: 85-93.
[12] Han W, Zhang C, Shi CT, Gao XJ, Zhou MH, Shao QX, Shen XJ, Wu CJ, Cao F, Hu YW, Yuan JL, Ding HZ, Wang QH and Wang HN. Roles of eIF3m in the tumorigenesis of triple negative breast cancer. Cancer Cell Int 2020; 20: 141.
[13] Nan L, Jacko AM, Tan J, Wang D, Zhao J, Kass DJ, Ma H and Zhao Y. Ubiquitin carboxyl-terminal hydrolase-L5 promotes TGFbeta-1 signaling by de-ubiquitinating and stabilizing Smad2/Smad3 in pulmonary fibrosis. Sci Rep 2016; 6: 33116.
[14] Huang MS, Yuan FQ, Gao Y, Liu JY, Chen YX, Wang CJ, He BM, Zhou HH and Liu ZQ. Circular RNA screening from EIF3a in lung cancer. Cancer Med 2019; 8: 4159-4168.
[15] Wang L, Wen X, Luan F, Fu T, Gao C, Du H, Guo T, Han J, Huangfu L, Cheng X and Ji J. EIF3B is associated with poor outcomes in gastric cancer patients and promotes cancer progression via the PI3K/AKT/mTOR signaling pathway. Cancer Manag Res 2019; 11: 7877-7891.
[16] Choe J, Lin S, Zhang W, Liu Q, Wang L, Ramirez-Moya J, Du P, Kim W, Tang S, Sliz P, Santisteban P, George RE, Richards WG, Wong KK, Locker N, Slack FJ and Gregory RI. mRNA circularization by METTL3-eIF3h enhances translation and promotes oncogenesis. Nature 2018; 561: 556-560.
[17] Goh SH, Hong SH, Lee BC, Ju MH, Jeong JS, Cho YR, Kim IH and Lee YS. eIF3m expression influences the regulation of tumorigenesis-related genes in human colon cancer. Oncogene 2011; 30: 398-409.
[18] Yan X, Hoek TA, Vale RD and Tanenbaum ME. Dynamics of translation of single mRNA molecules in vivo. Cell 2016; 165: 976-989.
[19] Jodoin R, Carrier JC, Rivard N, Bisaillon M and Perreault JP. G-quadruplex located in the 5'UTR of the BAG-1 mRNA affects both its cap-dependent and cap-independent translation through global secondary structure maintenance. Nucleic Acids Res 2019; 47: 10247-10266.
[20] Tan N, Dai L, Liu X, Pan G, Chen H, Huang J and Xu Q. Upregulation of caprin1 expression is associated with poor prognosis in hepatocellular carcinoma. Pathol Res Pract 2017; 213: 1563-1567.
[21] Shi Q, Zhu Y, Ma J, Chang K, Ding D, Bai Y, Gao K, Zhang P, Mo R, Feng K, Zhao X, Zhang L, Sun H, Jiao D, Chen Y, Sun Y, Zhao SM, Huang H, Li Y, Ren S and Wang C. Prostate cancer-associated SPOP mutations enhance cancer cell sur-

vival and docetaxel resistance by upregulating Caprin1-dependent stress granule assembly. Mol Cancer 2019; 18: 170.
[22] Zhang Y, You W, Zhou H, Chen Z, Han G, Zuo X, Zhang L, Wu J and Wang X. Downregulated miR-621 promotes cell proliferation via targeting CAPRIN1 in hepatocellular carcinoma. Am J Cancer Res 2018; 8: 2116-2129.
[23] Zhou Z, Yao X, Pang S, Chen P, Jiang W, Shan Z and Zhang Q. The deubiquitinase UCHL5/UCH37 positively regulates Hedgehog signaling by deubiquitinating Smoothened. J Mol Cell Biol 2018; 10: 243-257.
[24] Liu D, Song Z, Wang X and Ouyang L. Ubiquitin C-terminal hydrolase L5 (UCHL5) accelerates the growth of endometrial cancer via activating the wnt/beta-catenin signaling pathway. Front Oncol 2020; 10: 865.
[25] Zhang Z, Hu X, Kuang J, Liao J and Yuan Q. LncRNA DRAIC inhibits proliferation and metastasis of gastric cancer cells through interfering with NFRKB deubiquitination mediated by UCHL5. Cell Mol Biol Lett 2020; 25: 29.
[26] Chitta K, Paulus A, Akhtar S, Blake MK, Caulfield TR, Novak AJ, Ansell SM, Advani P, Ailawadhi S, Sher T, Linder S and Chanan-Khan A. Targeted inhibition of the deubiquitinating enzymes, USP14 and UCHL5, induces proteotoxic stress and apoptosis in Waldenstrom macroglobulinaemia tumour cells. Br J Haematol 2015; 169: 377-390.

Supplementary Table 1. The primer sequences used in qRT-PCR and RIP qRT-PCR

qRT-PCR primer name	primer sequence (5'-3')
CAPRIN1 (Forward)	GTTGAAACGGTTGAGGTG
CAPRIN1 (Reverse)	CATTTGTGCCATAAGGTC
TRAF6 F (Forward)	GGATGCCAAACCAGAGC
TRAF6 F (Reverse)	TCAAAGCGGGTGGAGAC
NUP160 (Forward)	GGTCTTACAAGGAGCAA
NUP160 (Reverse)	AAGGCAAAGTCAATCAG
CCNB3 (Forward)	GCTGCTGCCTCCTTACT
CCNB3 (Reverse)	CCCTGAGCCTCACAATC
PDHX (Forward)	CTGCTGCTAAAGGTATCCA
PDHX (Reverse)	GCATTTCCCTCTTCATCC
β-actin (Forward)	CACTGTGCCCATCTACGAGG
β-actin (Reverse)	TAATGTCACGCACGATTTCC

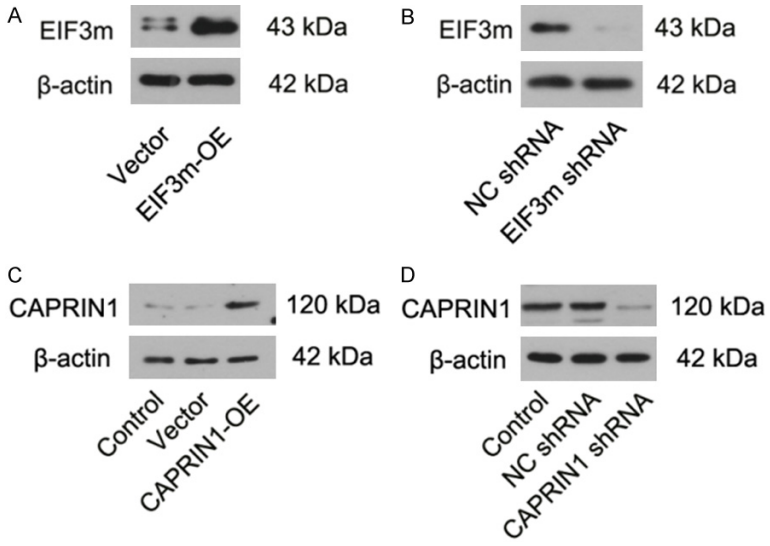

Supplementary Figure 1. The expression of EIF3m and CAPRIN1 was detected by western. The expression of EIF3m in xenograft tumor tissue was detected by western (A & B). The cells were transftected by CAPRIN1 over-expression or CAPRIN1 shRNA, the expression of CAPRIN1 was detected by western blot (C & D).

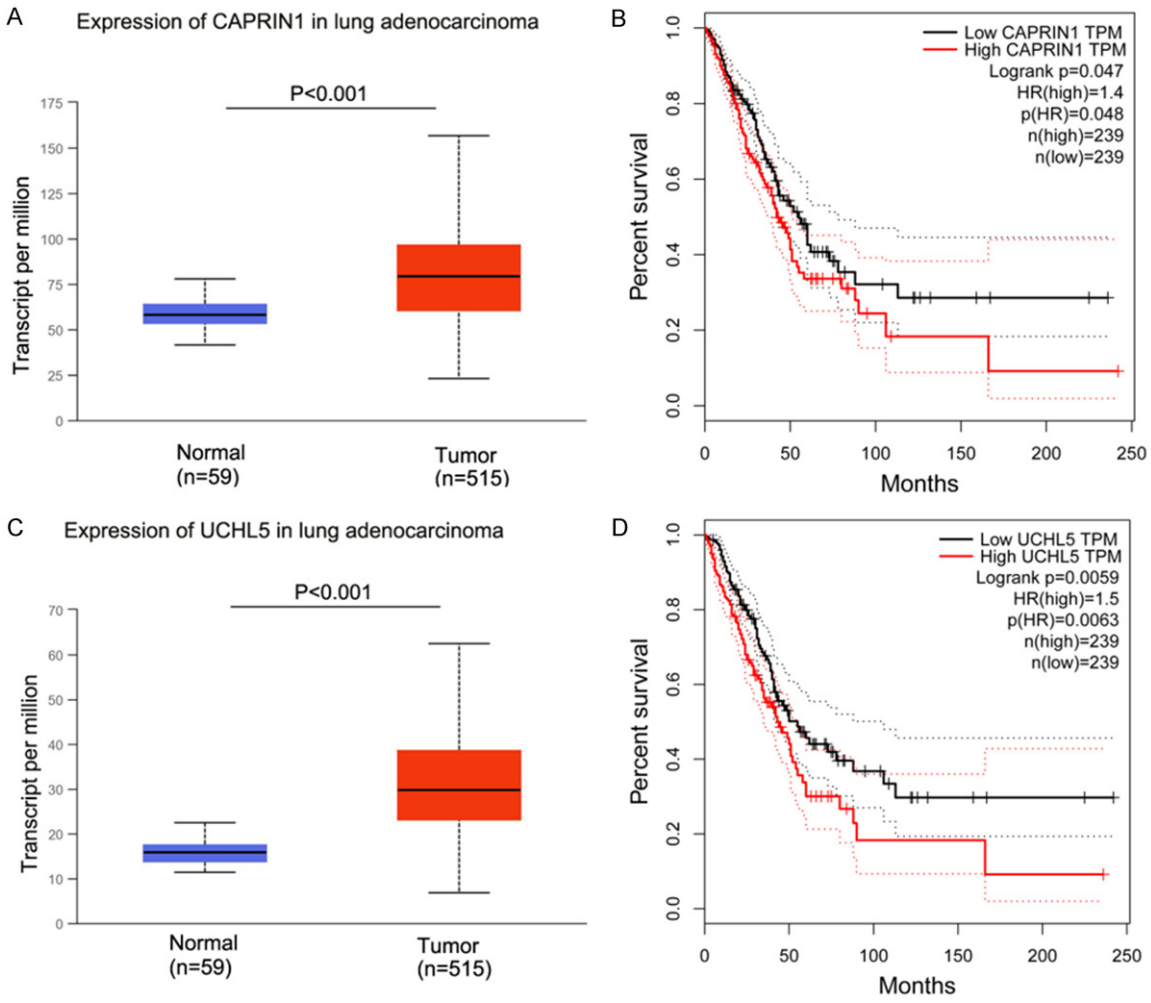

Supplementary Figure 2. Analysis of the expression of CAPRIN1 and UCHL5 from TCGA database. The expression of CAPRIN1 in normal and LADC tumor tissues (A) and the overall survival (B). The expression of UCHL5 in normal and LADC tumor tissues (C) and the overall survival (D).